A 3D eddy current model for the prediction of geometric image distortions in Stejkal-Tanner diffusion weighted EPI

K. R. O'Brien[1,2], N. Kickler[2], F. Lazeyras[1], R. Gruetter[2], T. Feiweier[3], and G. Krueger[4]

[1]Department of Radiology, Université de Genève, Geneva, Switzerland, [2]Laboratory for functional and metabolic imaging, Ecole Polytechnique Fédérale de Lausanne, Lausanne, Switzerland, [3]Siemens Healthcare Sector, Erlangen, Germany, [4]Advanced Clinical Imaging Technology, Siemens Suisse SA, Lausanne, Switzerland

Introduction: Recent hardware developments have greatly improved the eddy current (EC) performance on commercial MRI scanners. However, residual EC effects may still affect clinical applications when using EC sensitive acquisition schemes, such as the monopolar Stejkal-Tanner [1] diffusion weighted (DW) echo planar imaging (EPI). To overcome these limitations, less sensitive acquisition schemes [2] or retrospective correction based on time intensive EC-field measurements [3] or image registration, which is problematic at high b-values (b-value>1000s/mm^2) [4], may be used. Here, we aimed to evaluate the use of a "one time tune-up" phantom scan to predict the EC and geometric distortion i*n-vivo* for DW-EPI scans for retrospective correction.

Method & Results: All measurments were acquired on a 3T MRI scanner with a 32 channel head coil (Magnetom Trio a Tim System, Siemens Healthcare Sector, Erlangen, Germany).

3D-EC "tune-up" scan: 3D-EC field maps (TR/TE 150ms/10ms, Matrix 32x32, BW 390 Hz/pixel, 8mm isotropic voxel) were measured on a 190mm spherical phantom using established field mapping techniques [5]. The phase (ϕ) of each voxel represents the EC field caused by the test "DW" gradients; any phase alterations caused by other gradients are removed by subtracting the phase accrued in a second identical volume acquired with no test "DW" gradients. An estimate of the EC-field at each position in space was calculated offline ($B_{Eddy}(x,y,z) = \Delta\phi / \gamma TE$) (The MathWorks Inc., MA, USA).

	3D EC-field map	DW-EPI data sets High res.	DW-EPI data sets Clinical
δ (ms)	36.7	36.7	37.8 / 32.2
Δ (ms)	47.9	47.9	47.3 / 41.8
Direction	-1/0/0	0/0/±1	
	0/1/0	±1/0/0	
	0/0/-1	0/±1/0	±1/0.4/-0.4
	a/a/-b	±0.7/0/0.7	±1/0.4/0.4
	0.6/0.6/-0.4	0/0.7/±0.7	0.4/0.4/±1
	0.6/-0.4/0.6	0.7/±0.7/0	0.4/-1/±0.4
	-0.4/0.6/0.6	0.6/0.6/-0.4	-0.4/0.4/±1
		0.6/-0.4/0.6	-0.4/-1/±0.4
		-0.4/0.6/0.6	

Table 1 DW gradient attributes

Model development: Given i) most correction methods consider 0th (ε_0) and 1st (ε_{G^P} , ε_{G^R}) order EC corrections in k-space/image domain and ii) most DW studies acquire the volume as a stack of axial slices along the z-direction; the EC model was chosen to approximate the EC field as an axial stack of linear planes, $B_{Eddy}^{Model}(x,y,z) = \varepsilon_{G^R}.x + \varepsilon_{G^P}.y + \varepsilon_0$ where $\varepsilon_{0,G^R,G^P}(z) = f_x(z)G_X^{DW} + f_y(z)G_Y^{DW} + f_z(z)G_Z^{DW}$. To characterise the induced 3D EC-fields, the amplitude and direction of the DW gradients were varied according to Table 1, the duration (δ) & separation (Δ) were kept fixed. Figure 1(a-c) plots the mean and standard deviation, across a slice, of the 3D-EC field as a function of axial position. The slice mean of the 3D-EC-fields correlates with the DW gradient amplitude and exhibits a smooth spatial dependence with axial position. To capture this in the model, an axial position dependent quadratic weighting function ($f_{x,y,z}(z) = a_{x,y,z}z^2 + b_{x,y,z}z + c_{x,y,z}$) was incorporated and evaluated from the 3D-data using linear least squares minimisation. Figure 1(d-f) shows the residual mean and standard deviation of the EC-field after the 0th and 1st order EC-model's approximation is removed. The axial position dependence disappears and the standard deviation of the field reduces by ~60% leaving only residual error from higher order ECs, which translates in the high resolution protocol to a pixel shift of less than 0.2 pixels.

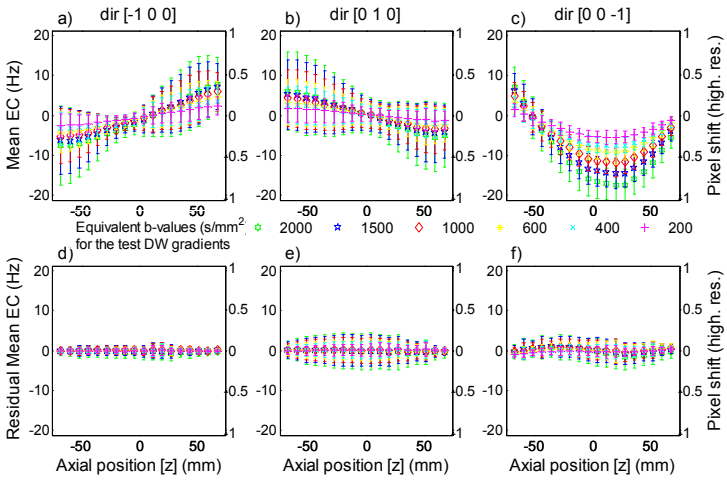

Figure 1: Mean and standard deviation in Hz (and pixel shift) of the measured (a-c) and residual (d-f) 3D EC field across a slice as a function of axial position (z) for gradient amplitudes that equate to a given b-value.

In-vivo acquisition: To verify the model's ability to predict EC *in-vivo*, b-value 600 and 1000s/mm^2 high resolution protocols (TR/TE 3600ms/102ms Matrix 128x96, 2x2x3mm voxel, GRAPPA factor 2, and BW 1502 Hz/pixel) and two typical b-value 1000s/mm^2 clinical protocols (TR 4800ms, Matrix 84x63, 2.5x.5x3mm voxel, GRAPPA factor 2 and BW 1384 Hz/pixel) at TEs of 102 and 92 ms were acquired with a prototype sequence using monopolar DW, directions in Table 1. Standard deviation images, before and after 0th and 1st order correction, figure 2, shows the variation of the signal intensity across the directions for each voxel. Similar to fractional anisotropy, a low standard deviation occurs in tissue with isotropic diffusion properties; high in tissues with a strong directional preference; and also high in regions of large distortions [6]. The distortions are particularly visible at tissue borders, (fig 2a-d). After correction, the regions of high standard deviation present at both anterior and posterior edges of the brain are visibly reduced. The image quality improves to that experienced in the twice refocused SE (fig 2c'/d' vs e).

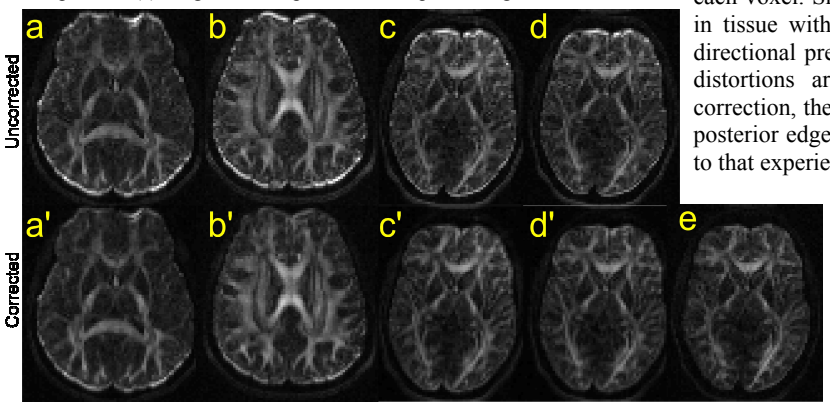

Figure 2: Standard deviation images of the monopolar DW scheme before (a-d) & after (a'-d') correction at isocentre (a), +13.5mm (b), +12.5mm (c-e) off centre– grayscale fixed by uncorrected image. (e) provides a twice refocused SE scheme for comparison.

Conclusions: The "tune-up" EC-model proposed provides a good approximation to the induced 3D EC field measured in a phantom. *In-vivo* geometric distortions are satisfactorily predicted for a range of DW gradients. With this EC model, image quality of the corrected *in-vivo* monopolar DW images improves and become comparable to the EC insensitive twice refocused SE [2] preferred clinically.

References: [1] Stejskal*l* 42(1965):288 J.Chem.Phys [2] Reese 49(2003):177 [3] Chen NeuroImage 30(2006):121 [4] Mohammadi. MRM 64(2010):1047 [5] Terpstra MRM 39(1998):139 [6] Finsterbush MRI 28(2009):434.